

# Calculating field emission currents in nanodiodes - a multi-group formalism with space charge and exchange-correlation effects

Debabrata Biswas and Raghwendra Kumar

*Theoretical Physics Division, Bhabha Atomic Research Centre, Mumbai 400 085, INDIA*

Inclusion of electron-electron interaction is essential in nano-diodes to understand the underlying physical phenomenon and tailor devices accordingly. However, both space charge and exchange-correlation interaction involve electrons at different energies and hence a self-consistent multi-energy-group solution of the Schrödinger-Poisson system is required. It is shown here that the existence of a limiting density-dependent potential at low applied voltages allows calculation of the field emission current. Despite additional interactions, a Fowler-Nordheim behaviour is observed. It is also found that the exchange-correlation potential dominates at these voltages in nanogaps and possibly leads to a higher turn-on voltage.

## I. INTRODUCTION

Nanotechnology has brought to the fore exotic materials such as carbon nanotubes and silicon nanowires that are being researched for a wide range of applications. Of particular interest is electron field-emission from nano materials that has potential to be used in vacuum electronics<sup>1</sup>, lithography and microwave power amplifiers<sup>2</sup>. Factors such as high efficiency, high current, low turn on voltages and fast turn-on times are being investigated for integration into existing devices. The necessity of an appropriate theoretical framework to deal with electron emission at the nanoscale is thus very important.

It is well known that field emission is an inherently quantum-mechanical phenomenon<sup>3</sup> governed by the Fowler-Nordheim (FN) law:

$$J = \frac{A}{\phi} (\mathcal{E}^2) \exp(-B\phi^{3/2}/\mathcal{E}) \quad (1)$$

where  $A$  and  $B$  are constants,  $\phi$  is the work function and  $\mathcal{E} = V_g/D$  is the applied electric field where  $V_g$  is the applied voltage and  $D$  the spacing between electrodes. A signature straight line fit in a  $\ln(J/V_g^2)$  vs  $1/V_g$  plot demonstrates that the simplified tunneling through a triangular-barrier model captures the essential physics, even though the calculated currents differ significantly from the observed ones.

Modifications to the law generally concentrate on the enhancement of the applied field<sup>4,5</sup> due to surface morphology and the image potential<sup>6-10</sup>. Most experimental studies characterize emitters using the effective work function and the enhancement factor  $\beta$  from an FN-plot with  $\mathcal{E}$  replaced by  $\beta\mathcal{E}$  in Eq. (1) above. However the fitted value of  $\beta$  and field enhancement calculations using observed surface morphologies seldom match<sup>11</sup>, leaving much scope for including physical phenomenon hitherto kept aside to maintain simplicity.

At the nanoscale especially, space charge and exchange-correlation potentials are important and can significantly alter the turn-on voltage. While these effects are small in a “standard” measure-theoretic sense

compared to the work-function, the image potential or the enhanced electrostatic potential, these slight changes in the barrier height or width can alter the transmission coefficient (and hence the emitted current) by orders of magnitude. These interactions however involve electrons at different energies so that the electron emission at the nanoscale is essentially a multi-energy group problem.

In the following, we shall formulate the field emission problem by including the space-charge and exchange-correlation potentials, discuss the challenges of multi-group emission and show that an alternate approach allows us to calculate the emission current at least at low applied voltages.

## II. FORMALISM

Field emission calculations that take into account electron-electron interaction generally involve a two-step process. In the absence of these interactions, the potential through which electrons tunnel into vacuum is independent of the current flowing through the gap. Thus, the density of electron states in the cathode and the transmission coefficient, both of which are known in-principle, determine the field emission current. When electron-electron interaction is turned on, the transmission coefficient depends on the current itself since the tunneling potential now depends on  $J$ . To deal with such a situation<sup>12</sup>, one may look for a solution to the equation

$$J = \frac{e}{2\pi\hbar} \int T(E, J) f(E) dE \quad (2)$$

where  $e$  is the electron charge,  $f(E)$  is the electron “supply function” within the emitter and  $T(E, J)$  is the transmission coefficient which in turn depends on the emission current density  $J$ . This requires (i) solving the Schrödinger-Poisson system to determine the self-consistent potential  $V_{eff}$  assuming that the wavefunction carries a given current density  $J$  and then (ii) using this potential to determine the transmission coefficient and thus the emission current density by computing the integral in Eq. (2). This process then can be repeated till a

solution is obtained.

As a first approximation, a single Schrödinger equation carrying a current  $J_k$  at an energy  $E_k$  may be coupled to the Poisson equation in order to determine  $V_{eff}$ , effectively implying that the calculation of the effective potential is performed assuming that all the electrons are at a single energy. More correctly, since the tunneling electrons are distributed across a range of energies, a multi-energy group approach needs to be adopted as we shall elaborate later. Even without this complication however, the approach outlined above is not guaranteed to lead to a solution to Eq. (2).

To understand this, note that a self-consistent solution of the 1-Schrödinger-Poisson system does not exist at any arbitrary value of  $J$ . In other words, there is a limiting mechanism that allows a self-consistent solution only upto a maximum current-density  $J_k^{max}$  at an energy  $E_k$ <sup>13–15</sup>. Note that at  $J_k^{max}$ , the tunneling electrons see a broader and higher effective potential barrier compared to values of  $J_k < J_k^{max}$ . Despite this, the integral in Eq. (2) evaluated using the effective potential at  $J_k^{max}$ , may lead to a value much larger than  $J_k^{max}$  depending on the supply function and the transmission coefficient. Thus, a solution to Eq. (2) may not exist especially in nano-diodes. Note that the problem is not linked to the use of a mono-energetic electron density in the Schrödinger-Poisson system. Rather, while a multi-energy group approach in solving the Schrödinger-Poisson system is necessary, it is generally the case that in nano-diodes, the exchange-correlation interaction lowers the maximum current density that can be supported in the diode resulting in a higher transmission coefficient<sup>16</sup>. The method for evaluating the field emission current at the nano level thus needs re-examination since a solution to Eq (2) may not exist.

Our formulation of the field emission problem for nano-diodes in the presence of electron-electron interaction is as follows: given an applied voltage  $V_g$  across the diode, the *maximum* current that can tunnel through and propagate across the gap in a self-consistent manner is the field-emission current. We shall use this definition in a multi-energy group formalism to determine the cold field emission current from metals.

In metals, electrons are distributed from the bottom of the conduction band to the Fermi level. It is thus necessary to divide the energy of the emitted electrons in the gap (vacuum) between the two metal electrodes, into  $N$  groups<sup>17</sup> and solve  $N$  Schrödinger equations, one for each energy group, coupled to each other through the Poisson equation and the exchange-correlation potential:

$$-\frac{\hbar^2}{2m} \frac{d^2\psi_k}{dx^2} + V_{eff}\psi_k = E_k\psi_k \quad (3)$$

$$\frac{d^2V}{dx^2} = \frac{e}{\epsilon_0}n(x) = \frac{e}{\epsilon_0} \sum_{k=1}^N |\psi_k(x)|^2. \quad (4)$$

Here,  $V_{eff} = \phi + V_{im} - eV + V_{xc} \times E_H$ , where  $\phi$  is the

work-function,  $E_H = e^2/(4\pi\epsilon_0 a_0)$  is the Hartree energy,  $a_0$  the Bohr radius and  $V_{im} = -e^2/16\pi\epsilon_0(x + x_0)$  is the image-charge potential with  $x_0$  such that  $\phi + V_{im} = 0$  at  $x = 0$ <sup>18,19</sup>. The exchange correlation potential<sup>20,21</sup>,  $V_{xc}$  in the local density approximation takes the form  $V_{xc} = \epsilon_{xc} - (r_s/3)d\epsilon_{xc}/dr_s$ , where  $r_s = [3/(4\pi n(x))]^{1/3}$  is the Wigner-Seitz radius,  $n(x)$  the electron number density,  $\epsilon_{xc} = \epsilon_x + \epsilon_c$  and  $\epsilon_x = -(3/4)(\frac{3}{2\pi})^{2/3} \frac{1}{r_s}$ ,  $\epsilon_c = \gamma/(1 + \beta_1\sqrt{r_s} + \beta_2 r_s)$  with  $\gamma = -0.1423$ ,  $\beta_1 = 1.0529$  and  $\beta_2 = 0.3334$ . The parametrized form for the correlation energy density,  $\epsilon_c$  is due to Perdew and Zunger<sup>21</sup>.

Note that  $V_{eff}$  refers to the self-consistent potential in the gap region between the two electrodes. Thus,  $V_{xc}$  is the exchange-correlation potential due to the electrons present in the gap while the image potential,  $V_{im}$ , is the linear response of the cathode<sup>19,22,23</sup> to the ‘external’ charges (steady state electrons) present in the gap. The ‘gap’ electrons in the vacuum region are thus modelled fully by the Kohn-Sham density functional theory and their only interaction with the cathode is due to the image potential<sup>24</sup>.

It is convenient to write the wavefunctions

$$\psi_k = \sqrt{n_0} q_k(x) \exp(i\theta_k(x)) \quad (5)$$

in terms of a real amplitude  $q_k(x)$  and phase  $\theta_k(x)$  and deal with equations for the amplitude  $q_k$ . Moreover, since we shall be dealing with scaled potentials and distance, it is necessary to frame the Schrödinger-Poisson system in dimensionless form<sup>13</sup> using the characteristic density  $n_0 = 2\epsilon_0 V_g / 3eD^2$ , the applied voltage  $V_g$ , the electron de Broglie wavelength  $\lambda_0 = \sqrt{\hbar^2 / 2meV_g}$ , the gap distance  $D$  and the Child-Langmuir current density  $J_{CL}$ <sup>28</sup>. In terms of the dimensionless normalized variables  $\bar{x} = x/D$ ,  $\bar{V} = V/V_g$ ,  $\lambda = D/\lambda_0$ ,  $\epsilon_k = E_k/eV_g$ ,  $\bar{J} = J/J_{CL}$ ,  $\bar{V}_{im} = V_{im}/(eV_g)$ ,  $\bar{V}_{xc} = V_{xc} \times E_H/(eV_g)$  and  $\bar{\phi} = \phi/(eV_g)$ , the  $N$ -Schrödinger and Poisson equations can be expressed respectively as

$$\frac{d^2 q_k}{d\bar{x}^2} = -\lambda^2 [\epsilon_k + \bar{V} - \bar{V}_{xc} - \bar{\phi} - \bar{V}_{im} - \frac{4}{9} \frac{\bar{J}_k^2}{q_k^4}] q_k \quad (6)$$

$$\frac{d^2 \bar{V}}{d\bar{x}^2} = \frac{2}{3} \sum_k q_k^2 \quad (7)$$

where  $k = 0, 1, \dots, N-1$ .

Eqns. (6) and (7) are complemented with appropriate boundary conditions for the potential  $\bar{V}$ <sup>25</sup> and the amplitude  $q_k$ <sup>15</sup>. Note that each of the wavefunctions  $\psi_k$  is assumed to carry a current density

$$J_k = \frac{e\hbar}{2mi} (\psi_k \frac{\partial \psi_k^*}{\partial x} - \psi_k^* \frac{\partial \psi_k}{\partial x}) \quad (8)$$

so that the equation for  $q_k$  is independent of  $\theta_k$ .

A set of currents  $\{J_k\}$  for which Eqns. (6) and (7) can be solved is a candidate for the field emission current

provided the emitter is able to emit the respective current densities  $J_k$  from each of the energy segments

$$J_k \leq \frac{e}{2\pi\hbar} \int_{E_k}^{E_k+\Delta} T(E)f(E)dE \quad \forall k \quad (9)$$

where the supply function  $f(E) = (mk_B T/\pi\hbar^2) \ln[1 + \exp((E_f - E)/k_B T)]^{3,9}$ . Here, the total integration domain  $[0, E_F]$  is divided into  $N$  equal energy segments of size  $\Delta$ . A solution set  $\{J_k\}$  yielding a valid  $V_{eff}$  normally satisfies Eqns. (9) in the nano regime. If the opposite holds (the inequality in Eq. (9) is not satisfied), the current will be “emission limited”.

In keeping with our formulation of the field emission problem, we are interested here in the maximal set of current densities  $\{J_k^{max}\}$  for which a solution of Eqns. (6) and (7) exists and  $J_k^{max}$  satisfies the emission inequalities. Determining this maximal set  $\{J_k^{max}\}$  by solving simultaneously  $N$  Schrödinger equations and the Poisson equation, and checking for its convergence is however a difficult task. We shall therefore take a different approach for determining the maximal set and hence the field emission current.

### III. THE EXISTENCE OF A LIMITING POTENTIAL

The maximal set defines a limit beyond which steady state electron flow ceases to exist. In other words, the time-independent Schrödinger-Poisson system no longer yields a solution beyond a limiting value for the current densities. Importantly, the limiting mechanism is expected to be universal in the low voltage “quantum regime” as well as at the high voltage “classical regime”<sup>15,26,27</sup>.

In the low voltage quantum regime, such a universality can reflect in the variable or density-dependent part of the effective potential comprising of the space charge and exchange-correlation potentials. To make a comparison, the scaled density-dependent voltage  $\bar{V}_{den} = (V_{xc} \times E_H/e - V)/V_g$  as a function of the scaled distance  $\bar{x}$  needs to be studied.

To test the universality hypothesis, consider emission at a single energy  $\epsilon_k$  (i.e.  $N = 1$ ). The maximum or limiting scaled current density at this energy,  $\bar{J}_s^{max}(\epsilon_k)$  (the subscript  $s$  denoting single energy group), can be determined by solving a single Schrödinger equation coupled to the Poisson equation self-consistently. If a universal limiting mechanism hypothesis holds, a plot of  $\bar{V}_{den}$  vs  $\bar{x}$  should be independent of  $\epsilon_k$  at  $\bar{J}_s^{max}(\epsilon_k)$ . This is true as shown in Fig. (1a) for  $D = 30\text{nm}$ ,  $V_g = 24.4\text{V}$  for  $E_k = 0$ ,  $-0.075$  and  $-0.15$ . The potentials are indeed identical. To check that the space charge and exchange-correlation potentials are not inconsequential at these low currents and charge densities, the scaled voltage  $\bar{V}_{den}$  is also compared at these parameters for  $\bar{J} = 10^{-10} \ll \bar{J}_s^{max}$  where  $J_{CL}$  is the Child-Langmuir current density<sup>28</sup>. At this

value of  $\bar{J}$ , the electron density is indeed negligible and  $\bar{V}_{den}$  expectedly does not bear the signature of the limiting potential.

The universality of this limiting potential is further tested by comparing  $\bar{V}_{den}$  at  $V_g = 25.4\text{V}$  and  $V_g = 24.4\text{V}$  for  $D = 30\text{nm}$  at their respective limiting current densities  $\bar{J}_s^{max}(E_k = 0; V_g)$ . The change in voltage does not affect the scaled limiting potential as seen in Fig. (1c).

Finally, in Fig. (1d) a comparison of two different systems is presented, one at  $D = 30\text{nm}$  and the other at  $D = 50\text{nm}$  for  $V_g = 24.4\text{V}$  and  $V_g = 40\text{V}$  respectively. In both cases, the scaled potential  $\bar{V}_{den}$  is obtained for limiting current density  $\bar{J}_s^{max}(0)$ . Clearly, the limiting potentials are very close and may be considered identical.

For a given gap spacing and applied voltage, the scaled effective potential  $\bar{V}_{eff} = V_{eff}/(eV_g)$  has in addition the scaled work-function  $\bar{\phi}$ , image potential  $\bar{V}_{im}$  and terms such as due to field enhancement (see section V), all of which are identical at a given gap spacing  $D$  and gap voltage  $V_g$  at all energies. Thus  $\bar{V}_{eff}$  should also reflect the universality observed in the density-dependent potential. This is shown in Fig. 1b.

### IV. THE MAXIMAL SET AND THE LIMITING FIELD EMISSION CURRENT

There is thus ample numerical evidence to state that a limiting potential exists which is independent of the electron energy when injection takes place at a single energy  $\epsilon_k$  with a current density  $\bar{J}_s^{max}(\epsilon_k)$ . Recall that beyond this maximal current, no solution exists for the 1-Schrodinger-Poisson system. The signature of the breakdown is the limiting potential.

It is therefore reasonable to put forward the hypothesis that even in multi-group emission, for the maximal set  $\{\bar{J}_k^{max}\}$ , the potential  $\bar{V}_{den}$ , assumes the universal 1-group limiting form observed in Fig. 1. Note that in each of the  $N$  equations in Eq. (6), the right hand side is identical to a 1-group limiting equation at energy  $\epsilon_k$  if  $\bar{J}_k^{max} = w_k \bar{J}_s^{max}(\epsilon_k)$  and  $q_k(\bar{x}) = \sqrt{w_k} q_s^{max}(\bar{x}; \epsilon_k)$  with  $w_k < 1$ . Here  $q_s^{max}(\bar{x}; \epsilon_k)$  is the 1-group amplitude at energy  $\epsilon_k$  and current density  $\bar{J}_s^{max}(\epsilon_k)$ . With such a scaling, each of the  $N$  Schrodinger equations assumes the respective 1-group limiting form at which steady state transmission ceases to exist.

Along with the  $N$  Schrödinger equations, the Poisson equation too should assume the 1-group limiting form. That such a form exists is borne out by plotting the 1-group amplitudes  $q_s(\bar{x}; \epsilon_k)$  at  $\bar{J}_s^{max}(\epsilon_k)$  for different injection energies. At the limiting current, the amplitudes  $q_s$  (and hence the charge density) assume a limiting form,  $q_s^{max}$  irrespective of the injection energy as can be seen in Fig. 2. In contrast, when  $\bar{J}_s(\epsilon_k) < \bar{J}_s^{max}(\epsilon_k)$ , the amplitude is far away from the limiting form as shown in Fig. 2.

In the multi-group case then, the Poisson equation can

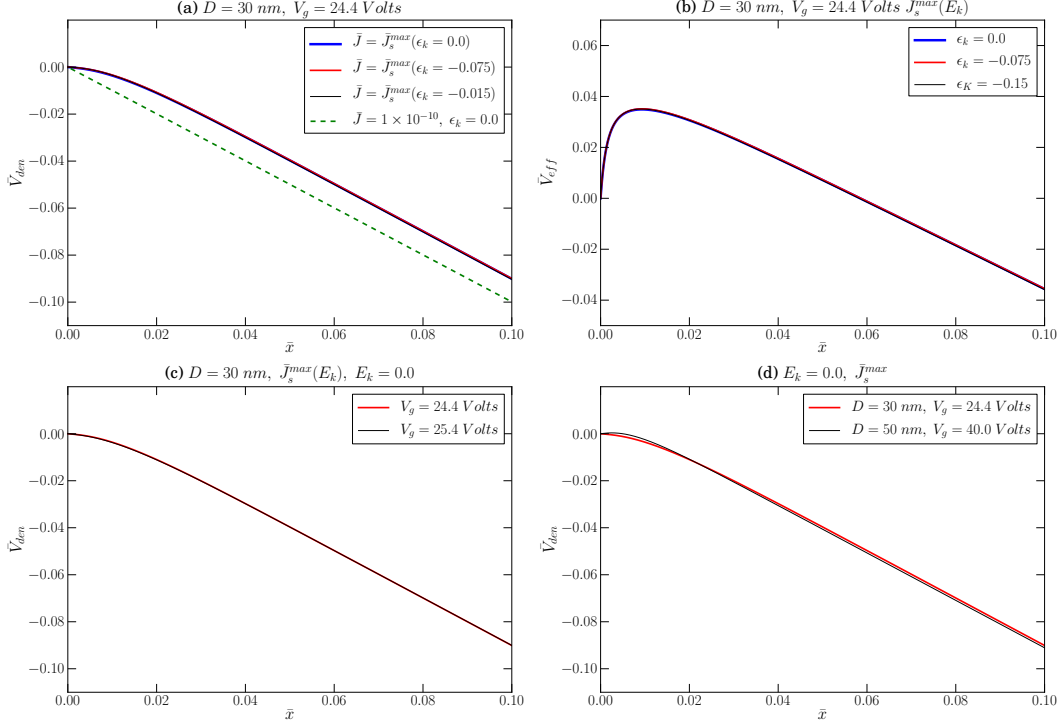


FIG. 1. The scaled density-dependent potential is shown as a function of the scaled distance  $\bar{x}$  in (a), (c) and (d). In (a), the dashed line corresponds to  $\bar{J} \ll \bar{J}_s^{max}(E_k = 0)$  while  $\bar{J}_s^{max}(E_k = 0) = 1.645 \times 10^{-6}$ ,  $\bar{J}_s^{max}(E_k = -0.075) = 4.6 \times 10^{-7}$  and  $\bar{J}_s^{max}(E_k = -0.15) = 1.3 \times 10^{-7}$ . In (b), the effective potential  $V_{eff}$  at  $D = 30\text{nm}$  and  $V_g = 24.4\text{V}$  is compared for three different injection energies. In (c),  $\bar{V}_{den}$  is compared for two different voltages at the same  $D$  while in (d) even the gap spacing is different. Note that  $\bar{x}$  varies from 0 to 1 and only a segment is shown to magnify the differences. The energies  $E_k$  are in units of  $eV$ .

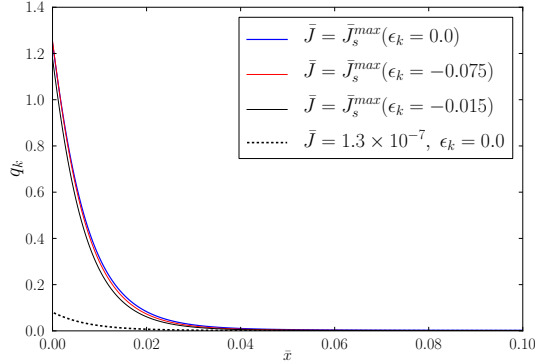


FIG. 2. The amplitude  $q_k$  at  $D = 30\text{nm}$  and  $V_g = 24.4\text{V}$  for different currents and injection energies. Note that  $q_k$  at  $\bar{J}_s^{max}(E_k = -0.15) = 1.30 \times 10^{-7}$  attains the limiting form while for the same current at a higher energy (dashed line),  $q_k$  is much smaller. The energies  $E_k$  are in units of  $eV$ .

be written as

$$\frac{d^2 \bar{V}}{d\bar{x}^2} = \frac{2}{3} \sum_k q_k^2(\bar{x}) = \frac{2}{3} \sum_k w_k (q_s^{max}(\bar{x}; \epsilon_k))^2 \quad (10)$$

when the  $N$  Schrödinger equations assume the 1-group limiting form. However, since  $q_s^{max}(\bar{x}; \epsilon_k) = q_s^{max}(\bar{x})$  is independent of  $\epsilon_k$ , we have

$$\frac{d^2 \bar{V}}{d\bar{x}^2} = \frac{2}{3} \sum_k w_k (q_s^{max}(\bar{x}))^2 = \frac{2}{3} (q_s^{max}(\bar{x}))^2 \sum_k w_k. \quad (11)$$

It then follows on demanding that the limiting multi-group electron density be identical to  $(q_s^{max}(\bar{x}))^2$ , that  $\sum_k w_k = 1$ .

Thus, with  $J_k = w_k J_s^{max}(\epsilon_k)$  and  $q_k(\bar{x}) = \sqrt{w_k} q_s^{max}(\bar{x})$ , each of the  $N$  Schrödinger equations together with the Poisson equation assume the limiting form where steady state transmission ceases to exist provided  $\sum_k w_k = 1$ . Thus  $\{w_k J_s^{max}(\epsilon_k)\}$  is the maximal set and the field emission current is

$$J = \sum_k w_k J_s^{max}(\epsilon_k). \quad (12)$$

It now remains to determine the weights  $w_k$ .

From a pure emission point of view, the current that can tunnel through a given potential,  $V_{eff}$ , in an energy segment  $\Delta$  at  $E_k$  is

$$(e/2\pi\hbar) \int_{E_k}^{E_k+\Delta} T(E)f(E)dE \simeq (e/2\pi\hbar)T(E_k)f(E_k)\Delta \quad (13)$$

if  $N$  is large enough. The weight of each segment is thus proportional to  $T(E_k)f(E_k)$ . When the potential in question is the limiting effective potential, the weight of each energy segment contributing to the charge density should again be proportional to  $T(E_k)f(E_k)$  where  $T(E_k)$  is computed using the limiting potential. Thus the normalized weights are  $w_k = T(E_k)f(E_k)/(\sum_k T(E_k)f(E_k))$  so that  $\sum_k w_k = 1$ . Since the limiting potential is known, the weights can be calculated and the field emission current determined. Typical plots of the weight at  $D = 30\text{nm}$  for two different applied voltages are shown in Fig. 3.

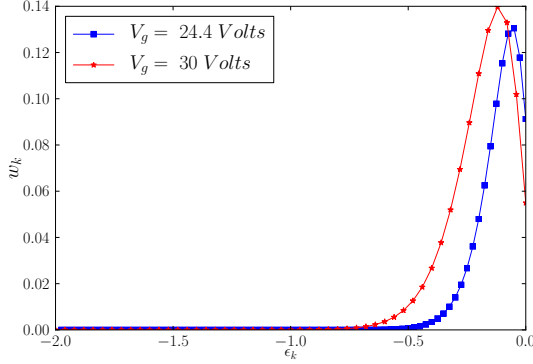


FIG. 3. The weights  $w_k$  for different injection energies at two different voltages. Here  $D = 30\text{nm}$ . The energies  $E_k$  are in units of  $eV$ .

Note that at higher applied voltages for a given nanogap (fixed  $D$ ), the limiting mechanism shifts and is increasingly dominated by the Poisson equation<sup>29</sup>. Arguments presented for the maximal set no longer hold in this domain.

## V. NUMERICAL RESULTS

We shall now use the prescription outlined in the earlier sections to determine the field emission current. The emitter used in this paper is Tungsten having  $\phi = 4.55\text{eV}$  and  $E_F = 10.46\text{eV}$ . Though the model used in this paper is 1-dimensional, we introduce field enhancement artificially to mimic a realistic situation, using a scaled applied potential based on the floating sphere model<sup>5,30</sup> by choosing the direction (angle  $\theta = 0$ ) along the gap. Thus, when no charge is present, the scaled applied potential is taken to be

$$\bar{V}_{enh}(x) = \frac{1}{4\pi\epsilon_0 V_g} \left[ -\frac{\mathcal{D}}{(x+\rho)^2} + \frac{\mathcal{C}}{(x+2h+\rho)} \right] + \frac{E_a}{V_g}(x+h+\rho)$$

$$-\frac{\mathcal{C}}{(x+\rho)} - \frac{\mathcal{D}}{(x+2h+\rho)^2}] + \frac{E_a}{V_g}(x+h+\rho)$$

where  $\rho$  is the radius of the sphere,  $h$  is the distance of the center of the sphere from the cathode,  $E_a = V_g/(D+h+\rho)$ ,  $\mathcal{C} = (4\pi\epsilon_0)E_a h \rho(1+\rho/2h)$  and  $\mathcal{D} = (4\pi\epsilon_0)E_a \rho^3$ . The values of  $\rho$  and  $h$  have been chosen to be  $0.1\text{nm}$  and  $5\text{nm}$  respectively. A comparison of the scaled applied potential with and without enhancement is shown in Fig. 4.

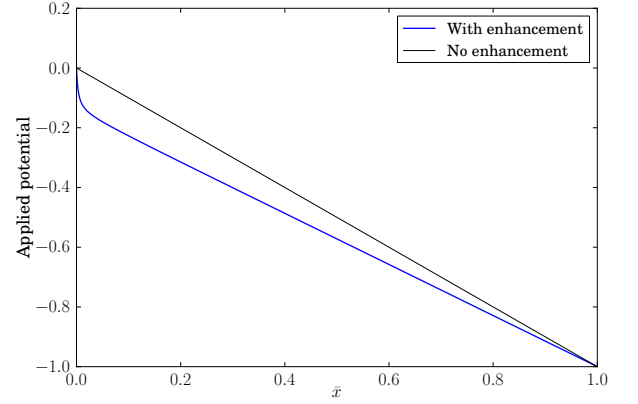


FIG. 4. A comparison of the scaled applied potential with (lower curve) and without (straight line) enhancement.

The limiting field-emission current density  $J$  calculated using Eq. (12) is shown in Fig. 5. Clearly, at lower voltages, the emission current follows an FN-curve as seen in experiments despite the fact that the current density shown here corresponds to the universal limiting potential. At higher voltages, the current density moves away from the FN-curve, coincident with the observation that  $\bar{V}_{den}$  moves away from the limiting potential thereby signalling a shift towards a limiting mechanism dominated increasingly by the Poisson equation. The current density should thus move towards the classical Child-Langmuir law<sup>28,31</sup> at high applied voltages.

The effect of the density-dependent potential in determining the limiting potential at lower voltages is striking. In its absence, the current density tunneling through the field-enhanced barrier is for example  $\bar{J} = 3.48 \times 10^{-4}$  at  $24.4\text{V}$  corresponding to  $\beta \simeq 7$  in the FN formula<sup>32</sup>. With the inclusion of the density dependent potential, the limiting current density drops to  $\bar{J} \simeq 5.19 \times 10^{-7}$  corresponding to a  $\beta \simeq 4.7$  in the FN formula.

The role of the space-charge potential in this lowering is insignificant at lower voltages since on removing the space-charge contribution, the limiting current density does not increase significantly. Thus, in nanogaps, the exchange-correlation potential plays a significant role and is likely responsible for the high turn-on voltages reported in literature for nanogaps as compared to microgaps<sup>33</sup>.



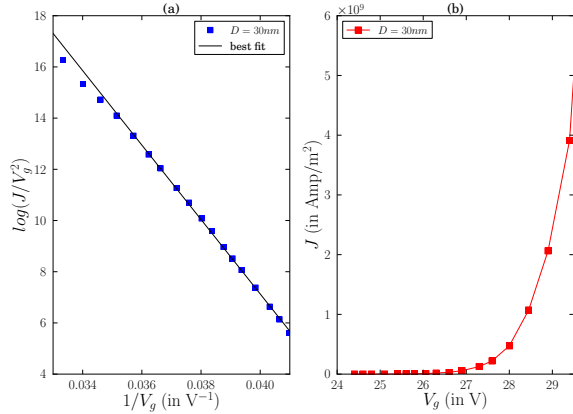


FIG. 5. The field emission current density evaluated using Eq. (12) for  $D = 30\text{nm}$ . In (a) an FN plot is shown along with the best fit  $f(1/V_g) = -1453.97 * (1/V_g) + 65.29$ . while (b) is a normal current density vs applied voltage plot.

## VI. CONCLUSIONS

In conclusion, we have provided a multi-energy-group formalism for calculating the field emission current in the presence of electron-electron interaction based on the existence of a limiting potential. We have found that at low voltages, the limiting emission current displays FN behaviour. The study also establishes that the exchange-correlation potential plays a significant role in lowering the emission current in nanogaps.

## VII. REFERENCES

- <sup>1</sup>Q. H. Wang, A. A. Setlur, J. M. Lauerhass, J. Y. Dai, E. W. Seelig, and R. P. H. Chang, Appl. Phys. Lett. **72**, 2912 (1998).
- <sup>2</sup>K. B. K. Teo, E. Minoux, L. Hudanski, F. Peauger, J.-P. Schnell, L. Gangloff, P. Legagneux, D. Dieumegard, G. A. J. Amaratunga, and W. I. Milne, Nature (London) **437**, 968 (2005).
- <sup>3</sup>R.H. Fowler and L. Nordheim, Proc. R. Soc. A **119**, 173 (1928).
- <sup>4</sup>R.G. Forbes, C.J. Edgcombe and U. Valdre, Ultramicroscopy **95**, 65 (2003).
- <sup>5</sup>X.Q.Wang, M.Wang, P.M.He, Y.B.Xu, and Z. H. Li, J. App. Phys. **96**, 6752 (2004).
- <sup>6</sup>L. Nordheim, Proc. R. Soc. A **121**, 626 (1928); E. L. Murphy and R. H. Good, Phys. Rev. **102**, 1464 (1956).
- <sup>7</sup>K.L.Jensen, J. App. Phys. **85**, 2667 (1999).
- <sup>8</sup>A.Rokhlenko, J. Phys. A: Math Theor., **44**, 055302 (2011);
- <sup>9</sup>K.L.Jensen J. Vac. Sci. Technol. B, **21**, 1528 (2003).
- <sup>10</sup>A.Rokhlenko, K.L.Jensen and J.L.Lebowitz, J. App. Phys. **107**, 014904 (2010).

- <sup>11</sup>H.Chen, Y.Du, W.Gai, A.Grudiev, J.Hua, W.Huang, J.G.Power, E.E.Wisniewski, W.Wuenssch, C.Tang, L.Yan, and Y.You, Phys. Rev. Lett. **109**, 204802 (2012).
- <sup>12</sup>W.Koh and L.Ang, Appl. Phys. Lett. **89**, 183107 (2006).
- <sup>13</sup>L. K. Ang, T. J. T. Kwan, and Y. Y. Lau, Phys. Rev. Lett. **91**, 208303 (2003).
- <sup>14</sup>D. Biswas and R. Kumar, Eur. Phys. J. B **85** 189 (2012).
- <sup>15</sup>D.Biswas and R.Kumar, Europhys. Lett. **102**, 58002 (2013).
- <sup>16</sup>At larger gaps however, the current may be emission limited at lower voltages since the exchange-correlation contribution is weak.
- <sup>17</sup>Ideally  $N \rightarrow \infty$ ; It is chosen to be large and convergence checked.
- <sup>18</sup>Bounds on  $x_0$  can be estimated based on the value of the metal exchange-correlation function in its bulk. Continuity at  $x = 0$  with the bulk value puts a lower bound with  $x_0$  determined by  $V_{im} + \phi + E_F = 0$ . A loose upper bound can be obtained from  $V_{im} + \phi = 0$ . The value of  $x_0$  for the field emission problem probably lies somewhere in between depending on the value of  $r_s$  at  $x = 0$ . We shall use the value of  $x_0$  from  $V_{im} + \phi = 0$ . This under-estimates the field emission current. For a discussion, see for instance<sup>19</sup>. The exact value of  $x_0$  is unimportant so far as the formalism presented here is concerned.
- <sup>19</sup>A. Kiejna, K.F. Wojciechowski, Metal Surface Electron Physics (Pergamon, Oxford, 1996).
- <sup>20</sup>W. Kohn and L. J. Sham, Phys. Rev. **140** A1133 (1965).
- <sup>21</sup>J.Perdew and A.Zunger, Phys. Rev. B **23**, 5048 (1981).
- <sup>22</sup>N.D. Lang and W. Kohn, Phys. Rev. B **7**, 3541 (1973).
- <sup>23</sup>The response of the anode is not modelled in this calculation since the gap  $D = 30\text{nm}$ .
- <sup>24</sup>Outside the unperturbed metal-vacuum interface, the asymptotic form of the exchange-correlation potential is image-potential like and the image charge is ascribed to the exchange-correlation hole that stays behind for an electron in the vacuum region<sup>19</sup>.
- <sup>25</sup>D. Biswas, Phys. Rev. Lett. **109**, 219801 (2012).
- <sup>26</sup>In the quantum regime, the limiting behaviour may be due to quantum reflection. See for instance<sup>15,27</sup>.
- <sup>27</sup>P. L. Garrido, S. Goldstein, J. Lukkarinen and R. Tumulka, Am. J. Phys. **79**, 1218 (2011).
- <sup>28</sup>C. D. Child, Phys. Rev. Ser. 1 **32**, 492 (1911); I. Langmuir, Phys. Rev. **2**, 450 (1913).
- <sup>29</sup>The contribution of the electrostatic potential  $\bar{V}$  in  $\bar{V}_{den}$  is negligible at lower voltages.
- <sup>30</sup>The choice of the enhanced potential is largely unimportant so far as the multi-group formalism is concerned.
- <sup>31</sup>R. R. Puri, D. Biswas and R. Kumar, Phys. Plasmas **11**, 1178 (2004).
- <sup>32</sup>The parameters in the floating-sphere model result in enhancement of the surface applied electric field (i.e at  $\bar{x} = 0$ ) by 53.5. This value decreases rapidly away from the surface. Note that for the range of energies at which emission takes place, the slope of the effective potential is smaller than 1 (see Fig. 1(b)). The transmission coefficient nevertheless increases since the barrier height away from the surface becomes smaller on including enhancement. Thus,  $\beta$  in the FN-formula exceeds 1.
- <sup>33</sup>T-C. Cheng, P-Y.Chen and S-Y. Wu, Nanoscale Res. Lett. (Springer), **7**, 125 (2012).